

## Supporting Information : Local Dynamics of Lignin

Derya Vural,<sup>1,2</sup> Catalin Gainaru,<sup>3</sup> Hugh O'Neil,<sup>4,5</sup> Yunquiao Pu,<sup>6</sup> Micholas Smith,<sup>1,5</sup> Venkatesh Sai Pingali,<sup>4</sup> Eugene Mamontov,<sup>7</sup> Brian H. Davison,<sup>8</sup> Alexei Sokolov,<sup>9</sup> Arthur J. Ragauskas,<sup>6,10</sup> Jeremy C. Smith,<sup>1,5</sup> and Loukas Petridis<sup>1,5</sup>

<sup>1</sup>*UT/ORNL Center for Molecular Biophysics,*

*Oak Ridge National Laboratory, P.O. Box 2008, Tennessee 37831 USA*

<sup>2</sup>*Department of Physics, Giresun University, Turkey, 28200*

<sup>3</sup>*Fakultät Physik, Technische Universität Dortmund, 44221 Dortmund, Germany*

<sup>4</sup>*Biology and Soft Matter Division, Oak Ridge National Laboratory,  
Oak Ridge, Tennessee 37831, USA*

<sup>5</sup>*Department of Biochemistry and Cellular and Molecular Biology,  
University of Tennessee, Knoxville, TN 37996, USA*

<sup>6</sup>*Joint Institute of Biological Sciences, Biosciences Division,  
Oak Ridge National Laboratory, Oak Ridge, TN 37830, USA*

<sup>7</sup>*Chemical and Engineering Materials Division,  
Oak Ridge National Laboratory, Oak Ridge, Tennessee 37831, USA*

<sup>8</sup>*Biosciences Division, Oak Ridge National Laboratory,  
Oak Ridge, Tennessee 37831, USA*

<sup>9</sup>*Chemical Sciences Division, ORNL, Oak Ridge, TN 37831, USA*

<sup>10</sup>*Department of Chemical & Biomolecular Engineering,  
University of Tennessee Knoxville, Knoxville, TN 37996, USA*

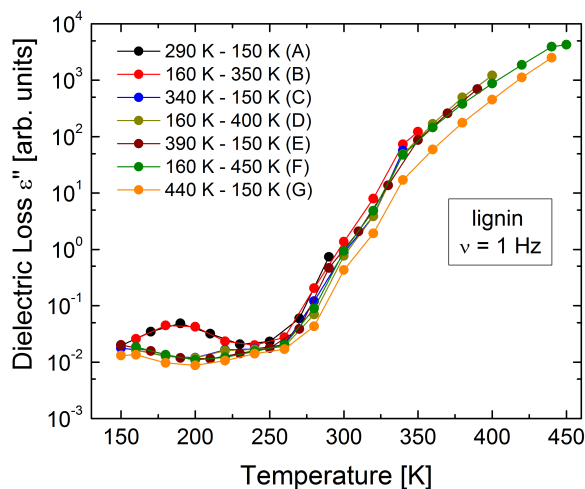


FIG. S-1: The dielectric loss  $\epsilon''$  (i.e. the imaginary part of the complex permittivity  $\epsilon^*$ ) of lignin measured at a single frequency of 1 Hz is plotted as function of temperature for the T-profile indicated in the legend, with the T-maxima reaching, consecutively, 290 K, 350 K, 400 K, and 450 K. Using this plot one can roughly estimate how different dielectric processes are affected by the thermal history and by the content of water in the sample. The most striking differences occur at low temperatures, much below the calorimetric glass transition: here for the first cooling cycle (A) data display a well-defined maximum which seems to vanish after the sample was heated to 350 K and cooled again. While the response does not change anymore for temperatures up to 400 K, a close inspection reveals some additional thermal history for the last cooling cycle (G) performed after the probe was heated up to 450 K.

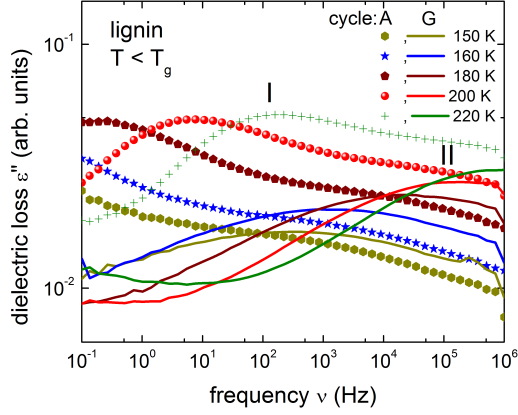


FIG. S-2: Focusing on the low temperature regime, the dielectric spectra recorded on A-cycle reveal the presence of two relaxation processes, denoted hereafter as I and II. However, after the sample was heated up to 450 K, only process II can be recognized for the data measured on cycle G. These results indicate that process I could be related to the presence of water in the sample, and only process II can be considered as a genuine secondary relaxation of neat lignin. The characteristic relaxation times for the two processes were calculated as  $\tau = 1/(2\pi\nu_{max})$ , where  $\nu_{max}$  is the characteristic frequency of the loss peak

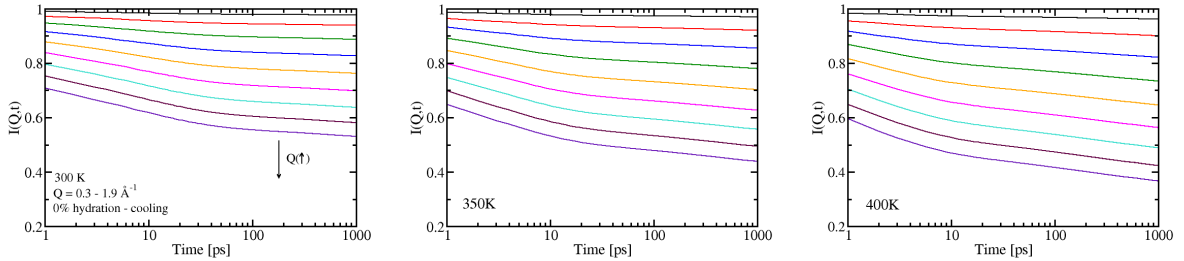


FIG. S-3: Incoherent intermediate scattering function  $I(Q,t)$ , calculated using Eq. (1), vs. time for 0% w/w hydration in cooling simulations at 300, 350 and 400 K.

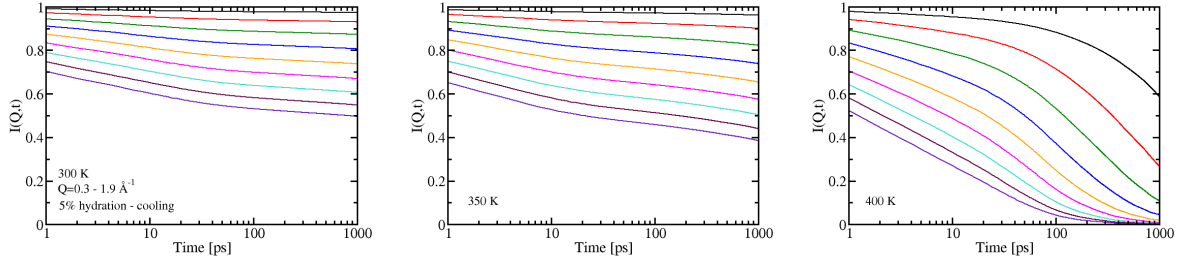


FIG. S-4: Incoherent intermediate scattering function  $I(Q, t)$ , calculated using Eq. (1), vs. time for 5% w/w hydration in cooling simulations at 300, 350 and 400 K.

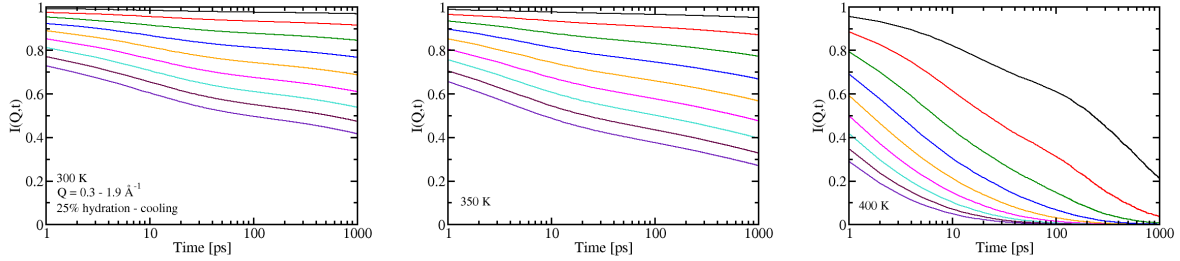


FIG. S-5: Incoherent intermediate scattering function  $I(Q, t)$ , calculated using Eq. (1), vs. time for 25% w/w hydration in cooling simulations at 300, 350 and 400 K.

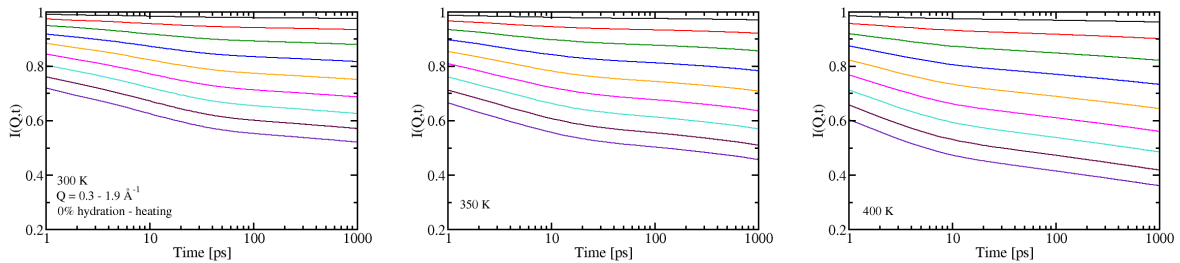


FIG. S-6: Incoherent intermediate scattering function  $I(Q, t)$ , calculated using Eq. (1), vs. time for 0% w/w hydration in heating simulations at 300, 350 and 400 K.

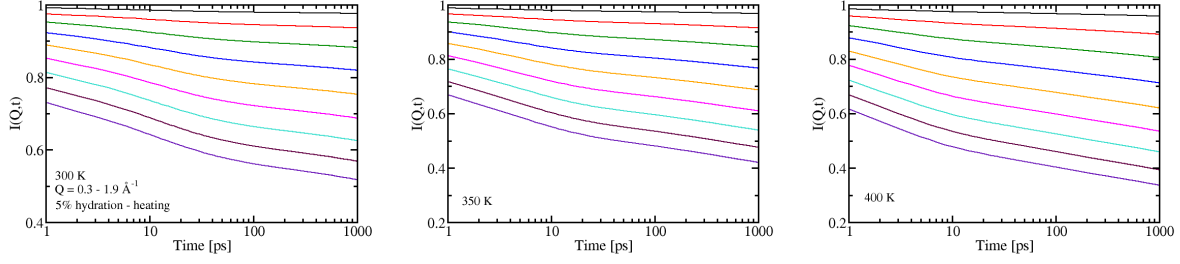


FIG. S-7: Incoherent intermediate scattering function  $I(Q, t)$ , calculated using Eq. (1), vs. time for 5% w/w hydration in heating simulations at 300, 350 and 400 K.

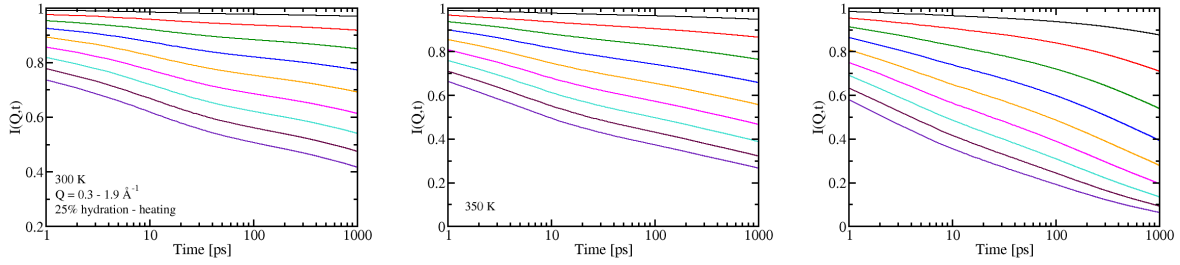


FIG. S-8: Incoherent intermediate scattering function  $I(Q, t)$ , calculated using Eq. (1), vs. time for 25% w/w hydration in heating simulations at 300, 350 and 400 K.

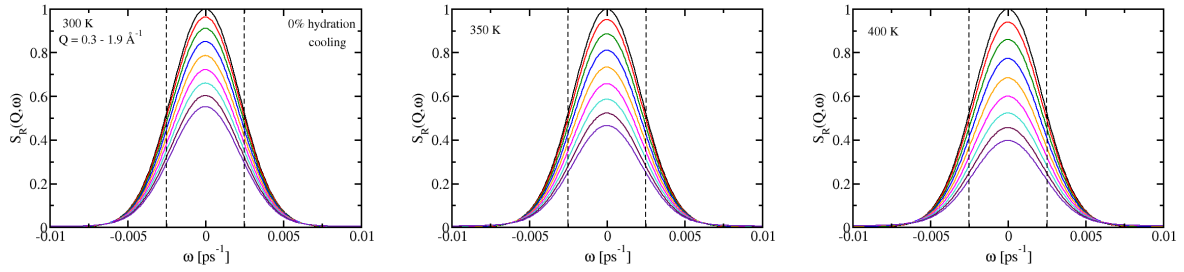


FIG. S-9: The scattering function  $S_R(Q, \omega)$  vs.  $\omega$  for 0%  $g_{water}/g_{lignin}$  hydration in cooling simulations at 300, 350 and 400 K. The Q-values from top to bottom are 0.3, 0.5, 0.7, 0.9, 1.1, 1.3, 1.5, 1.7 and  $1.9 \text{ \AA}^{-1}$ . The  $S_R(Q, \omega)$  is calculated by using Gaussian resolution function and  $I(Q, t)$  data (Figure S-3) in Eq. (3). The dashed lines represents the energy resolution of the BASIS spectrometer experiments:  $\omega \simeq 0.0025 \text{ ps}^{-1}$ , corresponding to  $E = 1.7 \text{ \mu eV}$ .

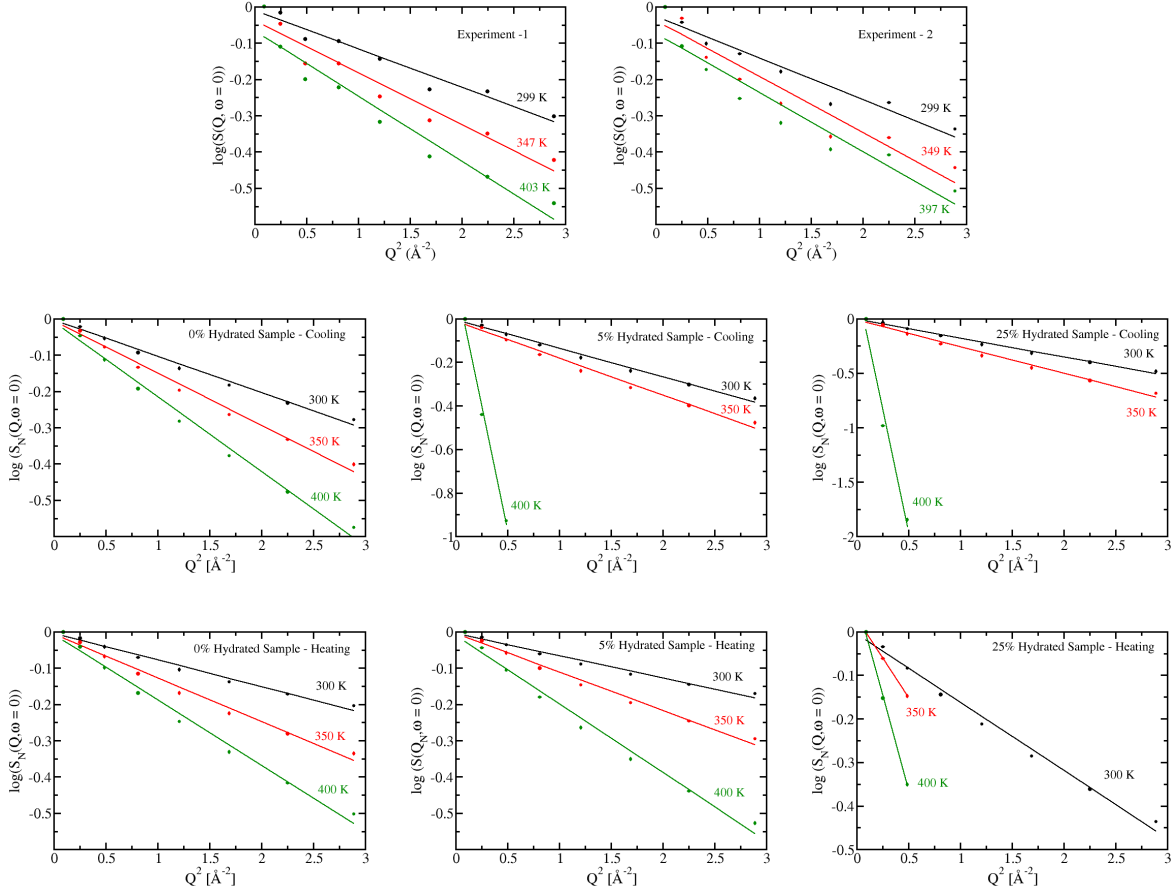


FIG. S-10: The normalized elastic component of the scattering function,  $S_N(Q, \omega = 0)$ , vs.  $Q^2$  at 300, 350 and 400 K obtained from QENS experiments (top row RHS: first heating circle, LHS: second heating circle) and heating and cooling simulations at three hydration levels,  $h = 0.0, 0.5$  and  $25 \text{ } g_{\text{water}}/g_{\text{lignin}}$ . The elastic component corresponds to the area under the  $S_R(Q, \omega)$  between the dashed lines in Figure S-9. Solid lines represent the fits of Eq. (4), used to obtain the MSD in Figure 4. The normalized intensity is defined as  $S_N(Q, \omega = 0) = \frac{S_R(Q, \omega=0, T) \times S_R(Q=0.3, \omega=0, T=150)}{S_R(Q, \omega=0, T=150) \times S_R(Q=0.3, \omega=0, T)}$ .

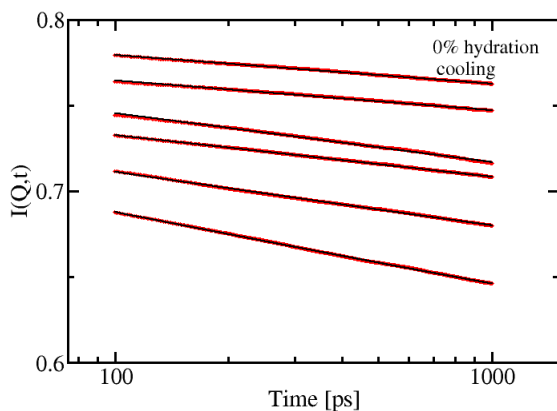


FIG. S-11: Stretched exponential function  $H + A \exp(-(t/\tau)^\beta)$  fits to the incoherent intermediate scattering function  $I(Q, t)$  for 0% w/w hydration in cooling simulations at 300, 320, 340, 360, 380 and 400 K to obtain the relaxation time,  $\tau$ , in Figure 3, where  $H$  is the plateau value,  $A$  constant,  $\tau$  the relaxation time and  $\beta$  the stretched exponential parameter.

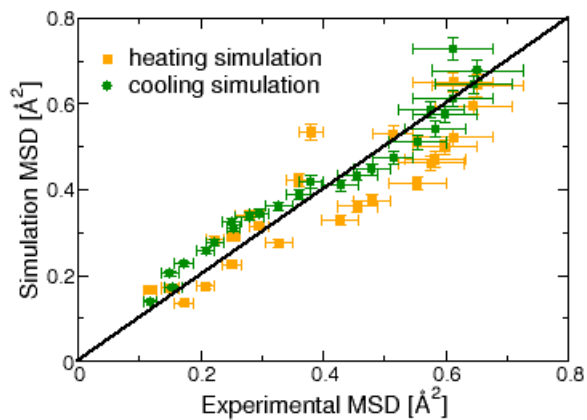


FIG. S-12: Comparison of the lignin mean square displacement obtained from MD simulation and experiment. Each point in the scatter plot represents the experimental and simulation-derived MSD at each temperature, with the respective uncertainties. The black diagonal line indicates perfect agreement.

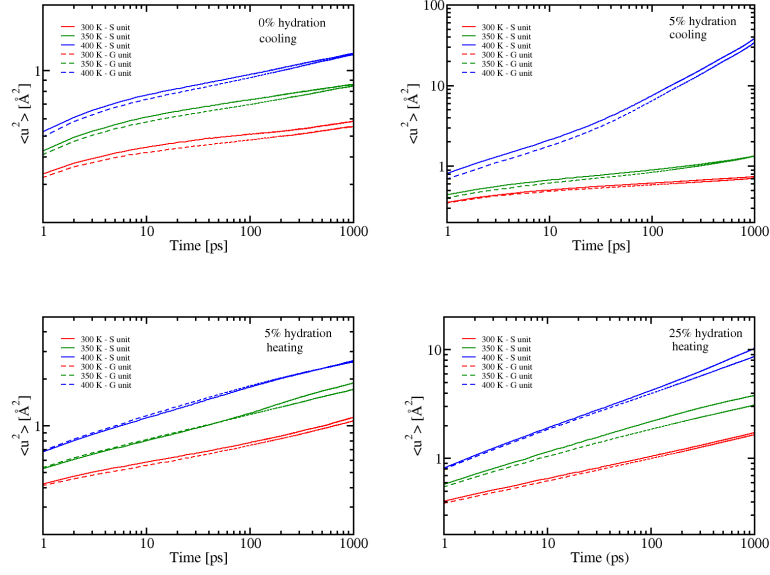


FIG. S-13: Mean square displacement vs. time calculated from the coordinates of all atoms in S-unit (solid line) and G-unit (dashed line) for cooling simulations at hydration level  $h = 0.0$  and  $h = 0.5 g_{water}/g_{lignin}$  and heating simulations at hydration level  $h = 0.5$  and  $h = 0.25 g_{water}/g_{lignin}$  and three temperatures, 300 (red), 350 (green) and 400 (blue) K.



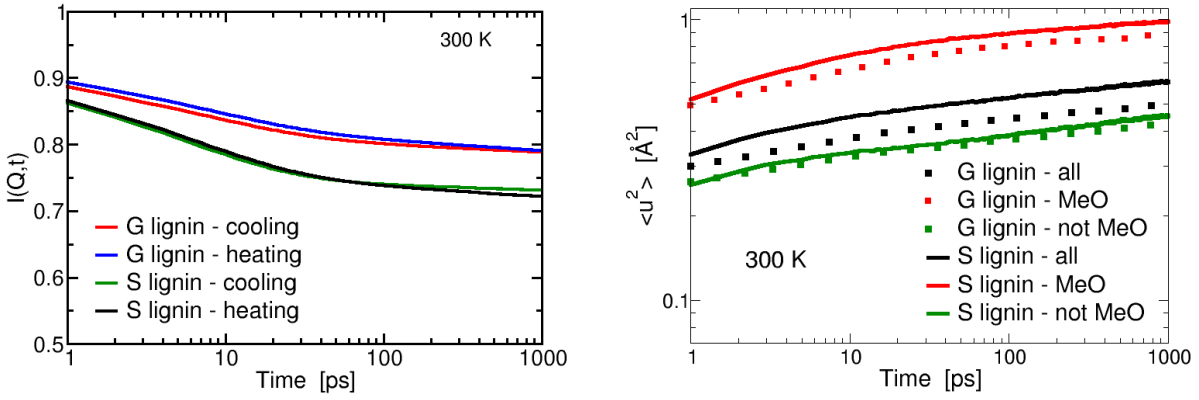


FIG. S-14: Comparison of the dynamics of lignin that contains only S or only G units at 300 K. The  $I(Q=1.1 \text{ \AA}^{-1}, t)$  calculated from heating and cooling simulations at 300 K indicate S-only lignin to be more dynamic than G-only. The mean square displacement, calculated from the heating simulations, is decomposed into contributions from methoxy (MeO) and non-methoxy atoms. We note the simulated systems in this Figure are different to those representative of vanilla lignin in Figure S-13.

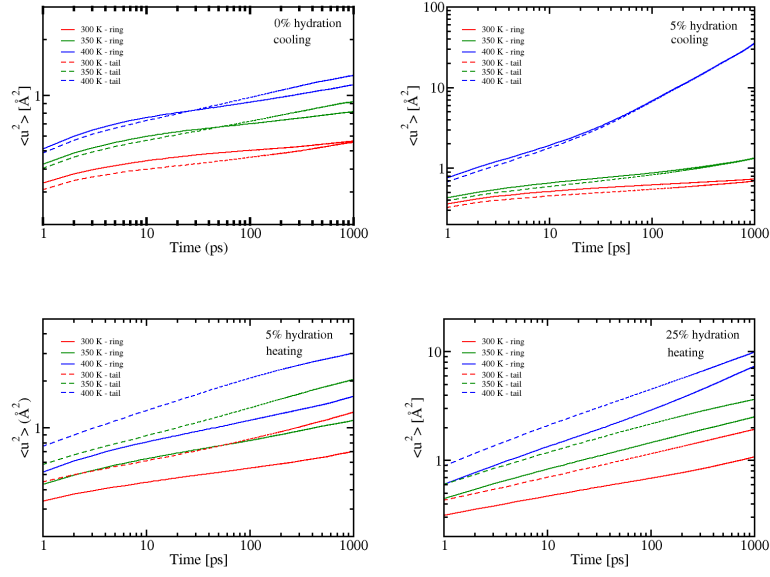


FIG. S-15: Mean square displacement vs. time calculated from the coordinates of all atoms in ring (solid line) and tail (dashed line) for cooling and heating simulations at hydration level  $h = 0.5$   $g_{water}/g_{lignin}$  and three temperatures, 300 (red), 350 (green) and 400 (blue) K.

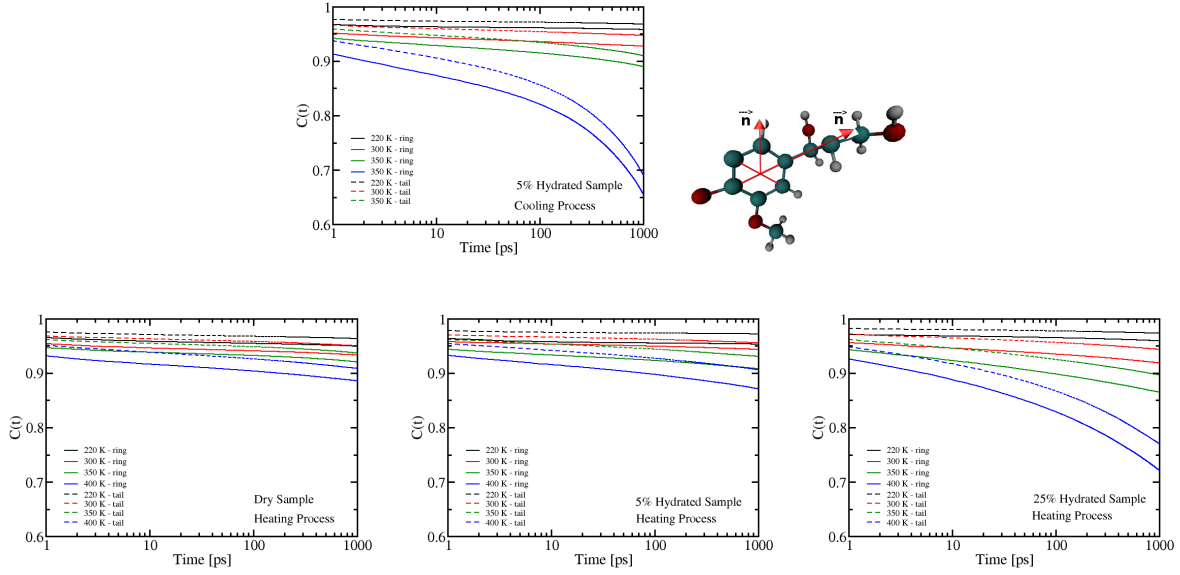


FIG. S-16: Orientational auto correlation function  $C(t)$  for ring (solid line) and tail (dashed line) moieties for three temperature, 300, 35 and 400 K: (Upper frame) cooling simulation for hydration level  $h = 0.5 g_{water}/g_{lignin}$  and (Lower frame) heating simulation for hydration level  $h = 0.0, 0.5$  and  $0.25 g_{water}/g_{lignin}$ . Lignin monomers can be considered to be made of two chemical moieties, a phenolic ring and a three-carbon aliphatic chain. To examine which moeity is more dynamic, we calculate the orientational autocorrelation function:  $C(t) = \langle \vec{n}(0) \cdot \vec{n}(t) \rangle$  where  $n$  is either the vector normal to the ring or the vector connecting the  $\alpha$  and  $\beta$  carbon atoms in the tail.  $C(t)$  is a measure of the loss of memory of the orietation of the lignin moieties, its steeper decay for the rings suggests their orientational dynamics are faster than for the tails. Comparison to  $I(Q, t)$  for the 25%-cooling sample at 400 K suggests that, above the glass transition temperature, lignin monomer translational dynamics, which dominate  $I(Q, t)$ , are faster than orientational dynamics, that dominate  $C(t)$ .

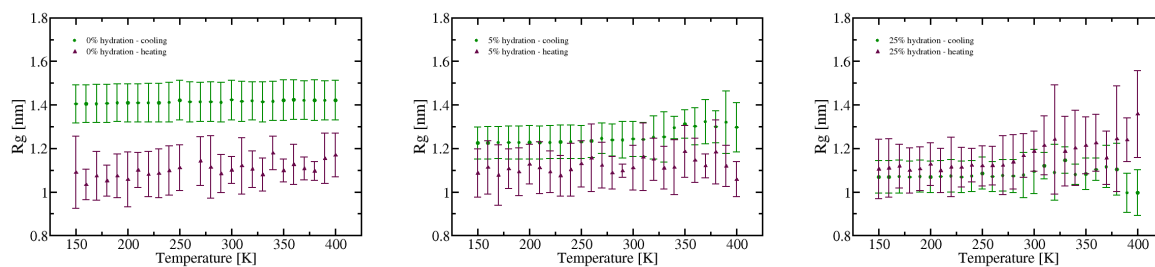


FIG. S-17: The lignin radius of gyration for heating and cooling simulations at three hydration level,  $h = 0.0, 0.5$  and  $0.25 g_{water}/g_{lignin}$ , used to obtain Figure 7.

TABLE S-1: The primary sequence of the first lignin molecule monomers linkages

S	
S	$\beta$ O4L
G	$\beta$ O4R
G	$\beta$ 5L
G	$\beta$ O4R
S	$\beta$ O4L
G	$\beta$ 5R
G	$\beta$ O4L
G	$\beta$ O4R
S	$\beta$ O4L
G	$\beta$ O4R
G	$\beta$ 5L
G	$\beta$ O4R
S	$\beta$ O4L
G	$\beta$ O4R
G	$\beta$ O4L
G	$\beta$ O4R
S	$\beta$ O4L
G	$\beta$ 5R
G	$\beta$ O4L
G	$\beta$ O4R
G	$\beta\beta$

TABLE S-2: The primary sequence of the second lignin molecule  
monomers linkages

S	
S	$\beta$ O4L
G	$\beta$ O4R
G	$\beta$ O4L
G	$\beta$ O4R
S	$\beta$ O4L
G	$\beta$ O4R
G	$\beta$ O4L
G	$\beta$ O4R
S	$\beta$ O4L
G	$\beta$ O4R
G	$\beta$ 5L
G	$\beta$ O4R
S	$\beta$ O4L
G	$\beta$ O4R
G	$\beta$ 5L
G	$\beta$ O4R
S	$\beta$ O4L
G	$\beta$ 5R
G	$\beta$ 5L
G	$\beta$ 5R
G	$\beta\beta$

TABLE S-3: The primary sequence of the third lignin molecule  
monomers linkages

S	
S	$\beta$ O4L
G	$\beta$ O4R
G	$\beta$ O4L
G	$\beta$ O4R
S	$\beta$ O4L
G	$\beta$ O4R
G	$\beta$ 5L
G	$\beta$ 5R
S	$\beta$ O4L
G	$\beta$ 5R
G	$\beta$ O4L
G	$\beta$ O4R
S	$\beta$ O4L
G	$\beta$ O4R
G	$\beta$ O4L
G	$\beta$ O4R
G	$\beta$ 5L
S	$\beta$ O4R
G	$\beta$ O4L
G	$\beta$ O4R
G	$\beta\beta$

TABLE S-4: The primary sequence of the fourth lignin molecule  
monomers linkages

S	
G	$\beta$ 5L
G	$\beta$ O4R
G	$\beta$ O4L
G	$\beta$ 5R
S	$\beta$ O4L
G	$\beta$ O4R
G	$\beta$ O4L
G	$\beta$ O4R
S	$\beta$ O4L
G	$\beta$ O4R
G	$\beta$ 5L
G	$\beta$ O4R
S	$\beta$ O4L
G	$\beta$ O4R
G	$\beta$ O4L
G	$\beta$ O4R
S	$\beta$ O4L
G	$\beta$ O4R
S	$\beta$ O4L
G	$\beta$ 5R
G	$\beta\beta$